# Solution-Processable Near-IR Photodetectors Based on Electron Transfer from PbS Nanocrystals to Fullerene Derivatives

By *Krisztina Szendrei, Fabrizio Cordella, Maksym V. Kovalenko, Michaela Böberl, Günther Hesser, Maksym Yarema, Dorota Jarzab, Oleksandr V. Mikhnenko, Agnieszka Gocalinska, Michele Saba, Francesco Quochi, Andrea Mura, Giovanni Bongiovanni, Paul W. M. Blom, Wolfgang Heiss,* and *Maria Antonietta Loi**

Research on high-performance, solution-processable semiconductors addresses the need for cheap mass production of electronic and optoelectronic devices. Organic semiconductors hold great promise owing to the inexpensive techniques used for their processing, though their low performance in terms of charge-carrier mobility and stability in ambient conditions, and the difficulty to obtain materials that absorb in the near-IR spectral range, are problems that need to be solved. Colloidal inorganic nanocrystals are emerging as valid substitute materials, because of their elevated stability in ambient conditions and the possibility of an extremely broad and tunable spectral response.[1–4] In particular, for applications requiring absorption and/or emission of light in the near-IR region of the electromagnetic spectrum, inorganic nanocrystals, especially those made of PbS and PbSe, show great advantages with respect to other solution-processable materials, as their fundamental absorption edge can be tuned, thanks to quantum confinement, in the wavelength range between 850 and 3500 nm.[3,5,6] These nanocrystals are synthesized in colloidal form by capping with a molecular-ligand shell, determining their solubility and limiting their charge-transport properties.[7,8] Their near-IR activity has been exploited in devices such as light-emitting diodes,[9,10] solar cells,[11,12] and photodetectors.[13,14] The latter show detectivity that outperform even epitaxially grown devices, when the ligand shell of the nanocrystal is manipulated after film preparation.[14] However, ligand manipulation results in strong power nonlinearity of the photodetectors[14] and fast degradation of the device performance.[15]

An alternative approach to the fabrication of photodetectors based on colloidal nanocrystals relies on blending inorganic nanocrystals in organic semiconducting matrices, such as polyphenylenevinylene derivatives,[16] polythiophenes,[17] and pentacene.[18] In devices such as hybrid solar cells[17,19,20] and photodetectors,[16,21] the nanocrystals act as electron acceptors, and the transport depends mostly on the hole-transporting properties of the polymers, resulting in strongly limited device performance.

Improvements in the overall device performance have been recently demonstrated, by using needlelike fullerene (C60) crystals photosensitized by nanocrystals.[22] The devices benefit from the higher carrier mobility in the C60 crystals than in the conjugated polymers. However, the performance of these devices does not nearly match that of the ligand-manipulated ones and, in addition, the needlelike crystals do not allow controllable device fabrication.

In this work, the hardly soluble C60 is replaced by its soluble derivative [6,6]-phenyl-C61-butyric acid methyl ester (PCBM), to obtain hybrid thin-film photodetectors with a spectral sensitivity covering the visible and near-IR spectral range up to 1300 nm, achieving performance close to that of commercial near-IR detectors. The active layer, which is composed of PbS nanocrystals and PCBM, exploits ultrafast charge transfer from the nanocrystals, which are fully covered by bulky oleic-acid ligands, to the fullerene, as indicated by time-resolved photoluminescence and by pump-and-probe measurements. Field-effect transistor measurements provided evidence that the electrons were the mobile carriers in the photodetectors, while the holes were trapped in the nanocrystals. Such a configuration allows photoconductive gain as well as a linear power dependence of the generated photocurrent. The measured detectivity compares to that of commercial photodetectors that are sensitive to near-IR radiation, making these hybrid devices appealing for applications in biology and in night-vision systems, as a cost-effective alternative to the currently available technology.

[*] Dr. M. A. Loi, K. Szendrei, Dr. F. Cordella, D. Jarzab, O. V. Mikhnenko, Prof. P. W. M. Blom
Zernike Institute for Advanced Materials
University of Groningen
Nijenborgh 4, Groningen, 9747 AG (The Netherlands)
E-mail: M.A.Loi@rug.nl
Dr. M. V. Kovalenko, Dr. M. Böberl, G. Hesser, M. Yarema, Prof. W. Heiss
Institute for Semiconductor and Solid State Physics
University of Linz
Altenbergerstr. 69, Linz 4040 (Austria)
A. Gocalinska, Dr. M. Saba, Dr. F. Quochi, Prof. A. Mura, Prof. G. Bongiovanni
Dipartimento di Fisica
Universitá degli Studi di Cagliari
S.P. Monserrato-Sestu km 0.7, Monserrato 09042 (Italy)

**DOI: 10.1002/adma.200801752**

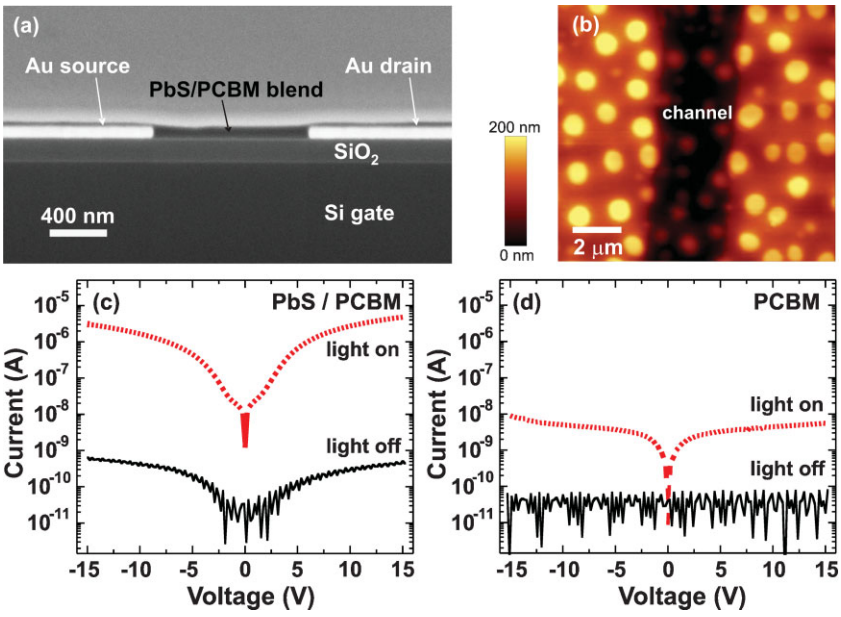


**Figure 1.** a) SEM cross-section of the field-effect transistor device. b) AFM image of the PbS/PCBM active layer on the electrodes and in the channel. c,d) Current–voltage (*I–V*) characteristics of the spin-coated PbS/PCBM blend and of PCBM thin films, respectively, under illumination (light on) and in the dark (light off).

Photodetectors were fabricated by spin-coating a thin film of PbS/PCBM blend (1:1 by weight) onto interdigitated gold electrodes with a 5 μm spacing. A cross-sectional scanning electron microscopy (SEM) image of the device is shown in Figure 1a; the morphology of the thin film as measured by atomic force microscopy (AFM) is shown in Figure 1b. The film appears as a homogeneous matrix embedding circular domains with diameters less than 1 μm and with heights of ca. 100 nm, which could not be ascribed to phase segregates by electron dispersive X-ray spectroscopy (EDX) and, thus, represent morphological features.

The *I–V* characteristics of the PbS/PCBM blend and of pure PCBM devices measured in the dark and under illumination are shown in Figures 1c and d. The *I–V* characteristics of both the hybrid blend and the PCBM thin-film devices are symmetric with respect to zero bias. The photocurrent of the blend has a linear dependence on the applied voltage for values less than 6 V, while at higher biases the dependence is quadratic. The hybrid device biased at 15 V under illumination with light of wavelength 514 nm at 6.0 mW $cm^{-2}$ produces a current of approximately $5 \times 10^{-6}$ A, while the dark current is four orders of magnitude less. This on/off ratio of $10^{-4}$ exceeds the reported on/off ratio for the C60-needlelike-crystal detectors by more than one order of magnitude.[22] The monochromatic quantum efficiency of the blended device at a bias of 15 V reaches up to 400%, indicating an amplification of the photocurrent.[14,23] The best responsivity value recorded for the hybrid devices exceeded 1.6 A $W^{-1}$ under illumination at 514 nm.

The reference device made of a pure PCBM film (Fig. 1d) showed a much weaker increase in current under illumination than the blend. At 15 V under homogenous illumination of 6.0 mW $cm^{-2}$, the device delivered a current of ca. $8 \times 10^{-9}$ A, while the dark current was ca. $5 \times 10^{-11}$ A (limited by the instrument sensitivity). The responsivity of the PCBM device was then $2.5 \times 10^{-3}$ A $W^{-1}$. Devices fabricated from pure PbS nanocrystals showed current bordering on the detection sensitivity of the experimental apparatus and did not perform any increment upon illumination; this is due to the insulating nature of the bulky ligand layer surrounding the nanocrystals.

To evaluate the responsivity to near-IR radiation, the photocurrent spectrum presented in Figure 2a was measured. The spectrum clearly shows a maximum at 1200 nm with a general shape that follows that of the optical density measured from a reference layer prepared by drop-casting on a glass substrate, which is shown in the same figure. The similar shape confirms the active role of the PbS nanocrystals in the photocurrent generation. The imperfect matching of the two spectra could be ascribed to the thickness difference in the films (drop-cast vs. spin-coated films).[24] The photocurrent at 514 nm is five times higher than at the first excitonic absorption peak of PbS, giving rise to a responsivity of 320 mA $W^{-1}$ at 1200 nm, which is still about 100 times the value reported for the best hybrid IR detectors.[16]

An important characteristic of photoconductive detectors is the power dependence of the photocurrent. A strong decrease in the responsivity on increasing power has been observed in pure nanocrystal photodetectors.[13,14] In contrast, the PbS/fullerene photodetectors reported here are characterized by an almost-linear response of the photocurrent with respect to the illumination power, from the nano- to the microwatt range, and both in the visible and in the near-IR regions of the electromagnetic spectrum (Figs. 2b, 2b inset). The linear response over several orders of magnitude is an important characteristic that renders these photodetectors appealing for several practical applications. The dynamic response of the blend photodetector is reported in Figure 2c; only 75% of the current disappears almost instantaneously when the light is switched off, while the rest of the current needs over 2 s to disappear. This is an indication of carrier trapping, which probably takes place at surface states of the colloidal nanocrystals. Long-living carrier trapping in the PCBM is ruled out because of the faster response observed in the pure PCBM reference sample (Fig. 2c). Furthermore, transport measurements on pure PCBM films revealed trap-free electron transport.[25]

The figure of merit for photodetectors is the normalized detectivity, defined as $D^* = (A\Delta f)^{1/2}R/i_n$, where $A$ is the effective area of the device, $\Delta f$ is the electrical bandwidth, $R$ is the responsivity, and $i_n$ is the noise current. In our photodetector, a noise current of ca. 0.28 pA $Hz^{-1/2}$ at 6 Hz was measured. This value decreased continuously to the limit of the experimental setup as the frequency was increased to 120 Hz. With the noise

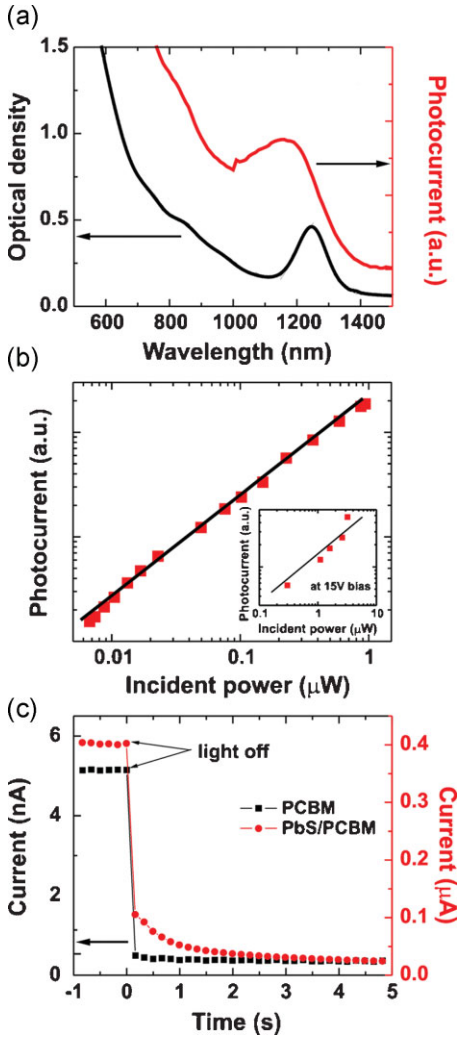


**Figure 2.** a) Optical density (black curve) and photocurrent spectrum (red curve) of a PbS/PCBM thin film. The photocurrent spectrum was measured at a bias of 25 V. b) Power dependence of the photocurrent under 1140 nm illumination. Inset: Power dependence of the photocurrent at 15 V bias under 514 nm illumination. c) Time behavior of the photocurrent of PCBM and PbS/PCBM thin films before and after switching off the illumination.

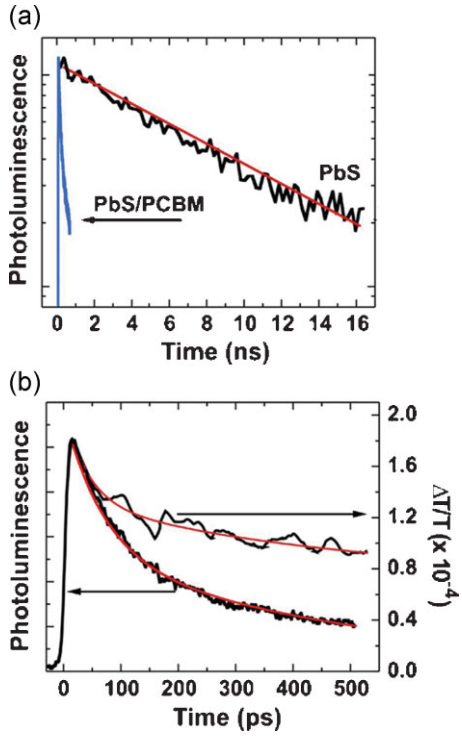


**Figure 3.** a) PL decay of the PbS nanocrystals and the PbS/PCBM thin film. The PL was excited at 800 nm. The decay was measured at the maximum of the PL spectrum at ca. 1350 nm. b) Pump–probe measurements on the PbS/PCBM blend (right axis) versus PL decay of the PbS/PCBM blend (left axis). The pump is at 784 nm and the probe at 1280 nm.

current measured at 6 Hz and the responsivity as given above, a detectivity $D^*$ of ca. $2.5 \times 10^{10}$ Jones (1 Jones = 1 cm $Hz^{1/2}$ $W^{-1}$) was obtained at 1200 nm. The noise-equivalent power (NEP) amounted to ca. 0.9 pW $Hz^{-1/2}$. These values are close to those achieved with the best commercial IR detectors operating at room temperature.

The physical mechanism enabling such improved performance of the photodetectors based on nanocrystals capped by oleic acid can be clarified by time-resolved optical spectroscopy performed on drop-cast films prepared on glass slides. Figure 3a compares the photoluminescence (PL) decays of the PbS nanocrystals and the PbS/PCBM blend thin films excited at 800 nm, where only the inorganic components absorb. The PL of the nanocrystals decays exponentially with a time constant of around 10 ns, while the PL of the blended thin film is quenched, showing a biexponential behavior consisting of a fast component, with a time constant of approximately 70 ps, and a slower component, with a time constant of approximately 580 ps, shown in detail in Figure 3b.

The much faster decay time of the PbS/PCBM emission can be attributed to an efficient charge transfer from the nanocrystals to the PCBM molecules. The exciton formed by photoexcitation of the nanocrystals can be separated, due to the high dielectric constant of the medium (3 nm PbS nanocrystals have a dielectric constant of ca. 16[26]) and the higher electron affinity of the fullerene derivative.

An important experimental tool used to distinguish and identify the dynamics of electrons and holes is the comparison of the time-resolved photoluminescence spectra and the transient-absorption spectra in pump–probe measurements. Figure 3b shows that the PL decay is faster than that of the transient absorption. While PL is a physical quantity that depends on the product of hole and electron populations, bleaching of the probe absorption induced by an ultrafast pump pulse depends on the sum of the hole and electron populations weighted by their relative contributions. One can therefore describe the pump–probe signal as the sum of a decaying component (caused by the carriers that are being transferred to the exterior of the nanocrystals) and a constant component (caused by the oppositely charged carriers remaining inside the crystals), which are approximately equal in magnitude. The photophysical experi-

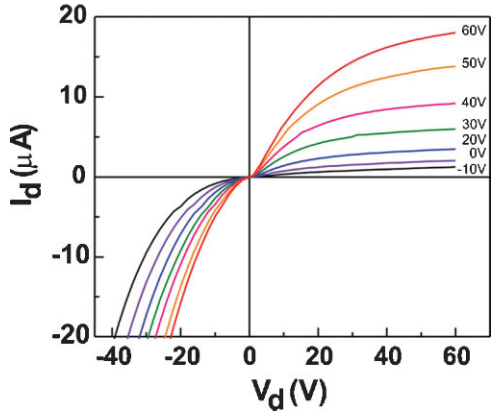


**Figure 4.** Output characteristics of a field-effect transistor with a PbS/PCBM blend as the active layer under illumination of 6 mW $cm^{-2}$ at 514 nm. $I_d$: drain current; $V_d$: drain–source voltage.

ments therefore provide evidence for charge transfer (as opposed to energy transfer) at the hybrid nanocrystal/fullerene interface.

The comparison of the relative energy levels of the conduction and valence bands of the nanocrystals and the highest occupied molecular orbital (HOMO)/lowest unoccupied molecular orbital (LUMO) levels of PCBM does not immediately indicate the possibility of any charge transfer between the two materials. An estimation of the energy levels for PbS nanocrystals emitting at 1280 nm derived from those of the bulk material gives the lowest unoccupied nanocrystal state at about 4.23 eV[27] below the vacuum level, and the highest occupied nanocrystal state at ca. 5.18 eV. Comparing these values with the LUMO and HOMO levels of PCBM, estimated to be approximately 4.2 and 6.0 eV below the vacuum level, respectively,[28] results in a close match of the unoccupied states of the PbS crystals and of PCBM. However, as previously reported, in colloidal nanocrystals the electronic states are found generally to be closer to the vacuum level than estimated from the bulk values,[29] rendering the transfer of electrons from the PbS to the PCBM energetically favorable. To verify this assumption, the hybrid blend films were investigated in a field-effect transistor configuration, which allowed the unambiguous assignment of the charge-carrier type dominating the transport in the photodetector devices.

The output characteristics of field-effect transistors whose active layers are thin films of a PbS-nanocrystal/PCBM blend are shown in Figure 4. The drain current is positive for positive drain–source voltages ($V_d$) and exhibits a saturation behavior, whereas at negative $V_d$ the current reverses sign and diverges. This behavior is characteristic of thin-film transistors with unipolar electron transport.[30] Furthermore, the devices exhibit strong gate dependence and electron-mobility values up to $3.0 \times 10^{-4}$ $cm^2$ $V^{-1}$ $s^{-1}$, as extracted from the linear regions of the transfer characteristics. This mobility value is ascribed to the PCBM, because transistors whose active layers consist of PbS nanocrystals capped with oleic acid do not operate.

In conclusion, the use of a solution-processable hybrid organic–inorganic blend of a fullerene derivative (PCBM) and PbS nanocrystals as the active medium in photodetectors was demonstrated. The active layer exploits photoinduced ultrafast charge transfer from the nanocrystals (which are fully covered by bulky oleic acid ligands) to the fullerene, demonstrating a new approach towards efficient photodetectors with respect to ligand manipulation. Field-effect transistor measurements proved that the electrons are the mobile carriers in the photodetectors, while the holes were trapped in the nanocrystals. In this configuration, photoconductive gain as well as a linear power dependence of the photocurrent was obtained. Moreover, the detectivity of these solution-processable devices compares well with that of commercial photodetectors sensitive to near-IR wavelengths, rendering them appealing, cost-effective alternatives to the currently available technology.

## Experimental

PbS crystals capped with oleic acid were synthesized according to a method reported in the literature [31]. The fullerene derivative PCBM was obtained from Solenne Bv (Groningen, The Netherlands). The samples for electrical measurements were spin-coated from a chlorobenzene solution (thickness ca. 100 nm) onto $Si/SiO_x$ substrates with interdigitated electrodes. For the field-effect transistor measurements, the active layer was spin-coated on heavily doped p-type Si substrates, which served as the gate electrode with 200 nm of thermally grown $SiO_2$ used as the dielectric layer, with a capacitance per unit area of 17 nF $cm^{-2}$. The source and drain electrodes consisted of 10 nm of Ti and 30 nm of Au. The samples for optical characterization were drop-cast (thickness ca. 1600 nm) onto quartz substrates from the same solution.

The sample cross-sections were inspected using a ZEISS 1540 XB cross-beam electron microscope. For this purpose, a Pt layer was first deposited with a focused ion beam. Next, a trench was sputtered using 20 keV Ga ions and the secondary electron images were taken using a 5 kV acceleration voltage and an in-lens detector.

The morphologies of the samples were determined by AFM in tapping mode.

Time-resolved PL measurements were performed by exciting the samples at 800 nm with a Ti:sapphire laser that provided 150 fs pulses. The PL emission was detected using a spectrometer coupled to a Hamamatsu streak camera with a cathode sensitive to near-IR radiation.

Differential transmission decays were obtained using a two-color pump–probe set up. The samples were excited by pulses from a regenerative amplifier (784 nm wavelength, 150 fs duration, 1 kHz repetition), and were probed with IR pulses (ca. 1280 nm wavelength) generated from a tunable-parametric amplifier. The pump beam, of 5 μW average intensity, was focused to a ca. 150 μm spot on the sample, corresponding to much less than one excitation per dot, in order to avoid shortening of the exciton lifetime by nonlinear processes; the probe sampled the inner half of the spot, to ensure homogeneous excitation.

Electrical measurements were carried out using a home-built probe station under high vacuum ($10^{-4}$ Pa) with a Keithley 4200 semiconductor analyzer at room temperature. To prevent parasitic currents and to electrically isolate the silicon substrate, a sheet of mica was used between the silicon substrate of the devices and the copper chuck. Illumination of the samples was provided by a 532 nm fiber-coupled laser, which allowed homogeneous illumination of the sample with a power of 6.0 mW $cm^{-2}$. The photocurrent was measured using a lock-in amplifier, and by illuminating the sample with a halogen lamp through an Acton monochromator (Spectra Pro 2150i).

## Acknowledgements

The work in Groningen and Cagliari was supported by the European Commission through the Human Potential Programs (RTN Nanomatch,

Contract No. MRTN-CT-2006-035884). The work in Cagliari was partially funded by MIUR through the FIRB project Synergy-FIRBRBNE03S7XZ. M.S. acknowledges the Italian Government Program ''Rientro dei Cervelli''. The Linz group is grateful for financial support from the Austrian Science Fund (FWF, projects START Y179 and SFB IRON).

Received: June 23, 2008
Revised: September 3, 2008
Published online: December 12, 2008

[1] C. Burda, X. Chen, R. Narayanan, M. A. El-Sayed, *Chem. Rev.* **2005**, *105*, 1025.
[2] M. Bruchez, M. Moronne, P. Gin, S. Weiss, A. P. Alivisatos, *Science* **1998**, *281*, 2013.
[3] J. M. Pietryga, R. D. Schaller, D. Werder, M. H. Stewart, V. I. Klimov, J. A. Hollingsworth, *J. Am. Chem. Soc.* **2004**, *126*, 11752.
[4] A. L. Rogach, A. Eychmüller, S. G. Hickey, S. V. Kershaw, *Small* **2007**, *3*, 536.
[5] M. V. Kovalenko, D. V. Talapin, M. A. Loi, F. Cordella, G. Hesser, M. I. Bodnarchuk, W. Heiss, *Angew. Chem. Int. Ed.* **2008**, *47*, 3029.
[6] E. Lifshitz, M. Brumer, A. Kigel, A. Sashchiuk, M. Bashouti, M. Sirota, E. Galun, Z. Burshtein, A. Q. Le Quang, I. Ledoux-Rak, J. Zyss, *J. Phys. Chem. B* **2006**, *110*, 25356.
[7] D. V. Talapin, C. B. Murray, *Science* **2005**, *310*, 86.
[8] Y. Yin, A. P. Alivisatos, *Nature* **2005**, *437*, 664.
[9] L. Bakuevaa, S. Musikhin, M. A. Hines, T.-W. F. Chang, M. Tzolov, G. D. Scholes, E. H. Sargent, *Appl. Phys. Lett.* **2003**, *82*, 2895.
[10] J. S. Steckel, S. Coe-Sullivan, V. Bulovic, M. G. Bawendi, *Adv. Mater.* **2003**, *15*, 1862.
[11] S. Zhang, P. W. Cyr, S. A. McDonald, G. Konstantatos, E. H. Sargent, *Appl. Phys. Lett.* **2005**, *87*, 233 101.
[12] K. W. Johnston, A. G. Pattantyus-Abraham, J. P. Clifford, S. H. Myrskog, D. D. MacNeil, L. Levina, E. H. Sargent, *Appl. Phys. Lett.* **2008**, *92*, 151 115.
[13] M. Böberl, M. V. Kovalenko, S. Gamerith, E. J. W. List, W. Heiss, *Adv. Mater.* **2007**, *19*, 3574.
[14] G. Konstantatos, I. Howard, A. Fischer, S. Hoogland, J. Clifford, E. Klem, L. Levina, E. H. Sargent, *Nature* **2006**, *442*, 180.
[15] G. I. Koleilat, L. Levina, H. Shukla, S. H. Myrskog, S. Hinds, A. G. Pattantyus-Abraham, E. H. Sargent, *ACS Nano* **2008**, *2*, 833.
[16] S. A. McDonald, G. Konstantatos, S. Zhang, P. W. Cyr, E. J. D. Klem, L. Levina, E. H. Sergent, *Nat. Mater.* **2005**, *4*, 138.
[17] W. U. Huynh, J. J. Dittmer, A. P. Alivisatos, *Science* **2002**, *295*, 2425.
[18] R. Thapa, K. R. Choudhury, W. J. Kim, Y. Sahoo, A. N. Cartwright, P. N. Prasad, *Appl. Phys. Lett.* **2007**, *90*, 252112.
[19] E. Arici, N. S. Sariciftci, D. Meissner, *Adv. Funct. Mater.* **2003**, *13*, 165.
[20] a) D. M. N. M. Dissanayake, A. A. D. T. Adikaari, S. R. P. Silva, *Appl. Phys. Lett.* **2008**, *92*, 093 308; b) D. M. N. M. Dissanayake, R. A. Hatton, T. Lutz, C. E. Giusca, R. J. Curry, S. R. P. Silva, *Appl. Phys. Lett.* **2007**, *91*, 133506-1.
[21] K. R. Choudhury, Y. Sahoo, T. Y. Ohulchanskyy, P. N. Prasad, *Appl. Phys. Lett.* **2005**, *87*, 073110.
[22] A. Biebersdorf, R. Dietmueller, A. S. Susha, A. L. Rogach, S. K. Poznyak, D. V. Talapin, H. Weller, T. A. Klar, J. Feldmann, *Nano Lett.* **2006**, *6*, 1559.
[23] C. Soci, A. Zhang, B. Xiang, S. A. Dayeh, D. P. R. Aplin, J. Park, X. Y. Bao, Y. H. Lo, D. Wang, *Nano Lett.* **2007**, *7*, 1003.
[24] V. Rinnerbauer, H.-J. Egelhaaf, K. Hingerl, P. Zimmer, S. Werner, T. Warming, A. Hoffmann, M. Kovalenko, W. Heiss, G. Hesser, F. Schaffler, *Phys. Rev. B* **2008**, *77*, 085 322.
[25] V. D. Mihailetchi, J. K. J. van Duren, P. W. M. Blom, J. C. Hummelen, R. A. J. Janssen, J. M. Kroon, M. T. Rispens, W. J. H. Verheea, M. M. Wienk, *Adv. Funct. Mater.* **2003**, *13*, 43.
[26] J. M. An, A. Franceschetti, A. Zunger, *Nano Lett.* **2007**, *7*, 2129.
[27] A. Maria, P. W. Cyr, E. J. D. Klem, L. Levina, E. H. Sargent, *Appl. Phys. Lett.* **2005**, *87*, 213112.
[28] C. J. Brabec, A. Cravino, D. Meissner, N. S. Sariciftci, T. Fromherz, M. T. Rispens, L. Sanchez, J. C. Hummelen, *Adv. Funct. Mater.* **2001**, *11*, 374.
[29] I. H. Campbell, B. K. Crone, *Appl. Phys. Lett.* **2008**, *92*, 043303-1.
[30] M. A. Loi, C. Rost-Bietsch, M. Murgia, S. Karg, W. Riess, M. Muccini, *Adv. Funct. Mater.* **2006**, *16*, 41.
[31] M. A. Hines, G. D. Scholes, *Adv. Mater.* **2003**, *15*, 1844.